Research Square

Preprints are preliminary reports that have not undergone peer review.
They should not be considered conclusive, used to inform clinical practice,
or referenced by the media as validated information.

Design and Synthesis of Benzylidene Phenylacetamide-based Derivatives as Potential Antibacterial Agents Targeting Staphylococcus Aureus Thymidylate Kinase

ABDUL BAQI
Sri Blaji Vidyapeeth School of Pharmacy
KOPPULA JAYANTHI
jayanthikoppula147@gmail.com

Sri Blaji Vidyapeeth School of Pharmacy
M MUTHUKUMARAN
Sri Blaji Vidyapeeth School of Pharmacy

Research Article

Keywords:

Posted Date: March 9th, 2026

DOI: https://doi.org/10.21203/rs.3.rs-9016290/v1

License: This work is licensed under a Creative Commons Attribution 4.0 International License.
Read Full License

Additional Declarations: Competing interest reported. no

DESIGN AND SYNTHESIS OF BENZYLIDENE PHENYLACETAMIDE-BASED DERIVATIVES AS POTENTIAL ANTIBACTERIAL AGENTS TARGETING *STAPHYLOCOCCUS AUREUS* THYMIDYLATE KINASE

MUTHUKUMARAN M[1], MOHD ABDUL BAQI [1], KOPPULA JAYANTHI [1*]

Department of Pharmaceutics, Sri Blaji Vidyapeeth School of Pharmacy, Karaikal, Pondicherry, India. muthuviyas@gmail.com (M.V) (Orcid id:0009-0003-0846-7684)

Department of Pharmaceutics, School of Pharmacy, Sri Blaji Vidyapeeth, Karaikal, Pondicherry, India. sufyan687@gmail (M.A.B) (Orcid id:0009-0000-3711-3568)

Department of Pharmaceutical Chemistry, Sri Blaji Vidyapeeth School of Pharmacy, Karaikal, Pondicherry, India. jayanthikoppula145@gmail.com (K.J) (Orcid id:0009-0003-9358-4278)

CORRESPONDING AUTHOR:

Dr. Koppula Jayanthi,

Associate Professor,

Department of Pharmaceutical Chemistry,
SBV School of Pharmacy, Karaikal,
Pondicherry, India,
Phone no: +919493953485,
Email: jayanthikoppula145@gmail.com,
Orcid id: 0009-0003-9358-4278

ABSTARCT

Objective : There has been a significant global surge in antimicrobial resistance in recent years, with Staphylococcus aureus infections proving particularly challenging to treat. The bacterium has resisted various antibiotics, including β-lactams. The primary objective is to identify antibacterial agents targeting *Staphylococcus aureus* Thymidylate kinase (TMK).

Methods: Six molecules were conceived through a process involving molecular docking (glide module), Qikprop screening for ADME (absorption, distribution, metabolism, and excretion) prediction, and prime MMGBSA (Molecular Mechanics Generalized Born Surface Area) analysis to assess binding free energy employing Schrödinger suite 2021-4. in-*vitro* studies MIC, MBC, and TIME KILL were performed to evaluate the antibacterial activity. The designed molecules are evaluated based on glide score binding affinity and *in-vitro* results.

Findings: The six molecules exhibited hydrophobic and hydrogen bonding interactions with the *Staphylococcus aureus* Thymidylate kinase (4HLC.pdb). Thymidylate kinase (TMK) enzyme, as identified in the Protein Data Bank entry. Among these, compound C_3 displayed XP-docking Glide score and ΔBind of -4.39 kcal/mol and -76.93 kcal/mol respectively. To explore the dynamic behaviour of the C_3/4HLC complex, a 100-nanosecond molecular dynamics simulation was conducted. Gram-positive strains of *S. aureus* (NCIM 5021) Ic_{50} values (1.91 µM), clinical *MRSA* strains (ATCC 43300) Ic_{50} values (3.91 µM) shown in the in-vitro study.

Interpretation: Based on all studies in the performance of C_3 demonstrated with favourable outcomes, Benzylidene phenyl acetamide-based derivatives are anticipated to be potential future inhibitors of the *SATMK*, suggesting their potential role as antibacterial agents.

Funding: We have no funding for this project.

INTRODUCTION

In recent years, the surge in infections from multidrug-resistant bacterial pathogens has become a critical concern for public healthcare. Prolonged misuse of antibiotics has led to the emergence of resistant strains like *Staphylococcus aureus, Neisseria gonorrhoeae, Escherichia coli, and Mycobacterium tuberculosis*. Unfortunately, attempts to develop new antibiotics have not kept pace with the rise of these antibiotic-resistant strains. Urgent and intensified antibiotic research and development efforts are imperative to counter the escalating threat of antimicrobial resistance in healthcare effectively.[1] *Staphylococcus* infections pose a significant threat to public health, especially among older adults, as these bacteria can lead to various conditions, such as cellulitis, *pneumonia*, skin infections, and *bacteremia*.[2] Unfortunately, the emergence of antibiotic resistance, including resistance to β-lactam antibiotics and *vancomycin*, has complicated the treatment of these infections. To address this issue, the development of new antibiotics is crucial.[3] Thymidylate kinase (TMK) has recently gained attention as a potential target due to its significant role in cell proliferation.[4] This enzyme catalyzes the conversion of deoxythymidine monophosphate (dTMP) to deoxythymidine diphosphate (dTDP), which then further converts to deoxythymidine triphosphate (dTTP), a key component in DNA formation. (figure 1).

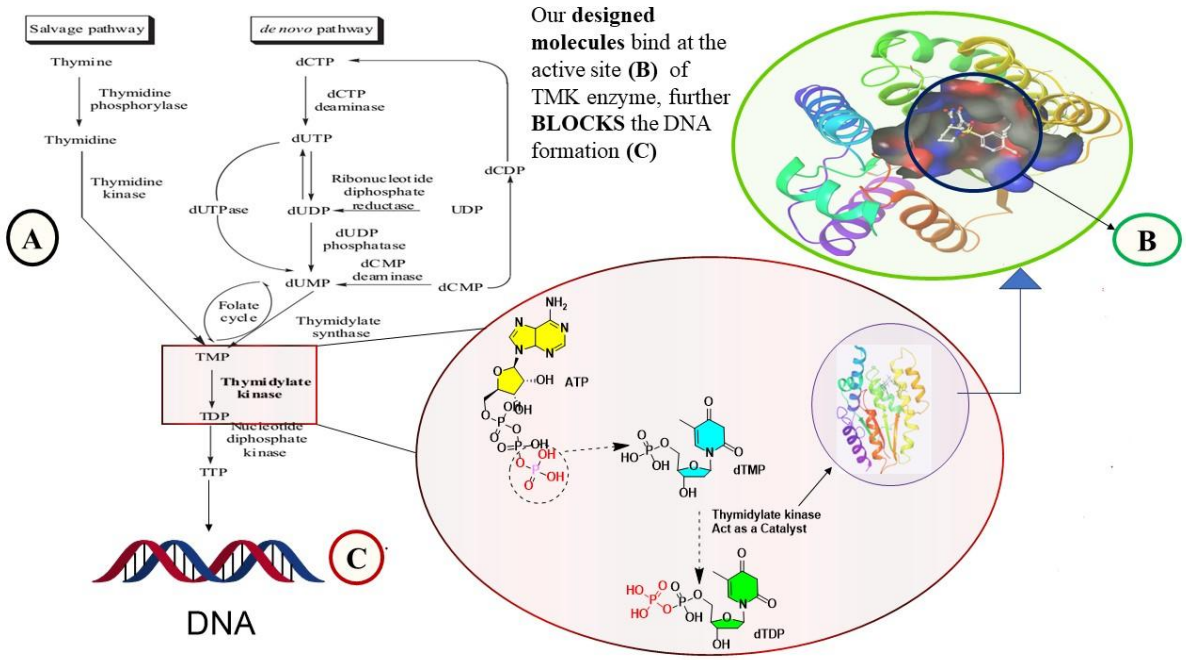


Figure 1. Thymidylate kinase's role in DNA synthesis

TMK is present in humans and bacteria, including notable pathogens like *Mycobacterium tuberculosis, Pseudomonas aeruginosa, Bacillus anthracis, Staphylococcus aureus*, and *Escherichia coli*.[5]*Staphylococcus aureus thymidylate kinase* (*SaTMK*) is particularly interesting as a target, given its unique characteristics compared to other bacteria and *Human TMK* (*HaTMK*). The consensus sequence difference between eukaryotic and prokaryotic forms, specifically in the P-loop, makes *SaTMK* an attractive focus for developing selective inhibitors.[6,7] The elucidation of the TMK X-ray structures of both human [8] and *S. aureus* [9] and their low (19%) sequence homology enhances the consideration of TMK as an attractive target for developing selective inhibitors. Two classes of TMKs have been identified: Class I enzymes are mainly from eukaryotes and have an arginine residue in position x_1 of the consensus sequence Gxxx$_1$xGKx of the P-loop, which interacts with ATP. class II TMKs are of prokaryotic origin and can be distinguished by the presence of a glycine residue instead of arginine in the x_1 position of the consensus sequence, along with additional basic residues (mostly Arg) in the LID region that interact with ATP. Inhibitors may thus potentially be designed to specifically target prokaryotic TMKs without affecting the host (human) enzyme, with the expectation that toxicity for the host can be minimized. Inhibitors can be designed targeting the regions of the TMP site conserved between the various bacterial TMKs but with structural differences to that of human thymidine monophosphate kinase (TMK) to obtain broad-spectrum antibacterial agents. The possibility would be to design inhibitors containing hydrogen-bonding groups targeting Arg36, Arg48, and Arg70 at the base of the TMP-binding cavity of *Sa*TMK, an interaction not formed by other TMKs containing proline in this position of the active site. In the present work, we aimed to target Arg36, Arg48, and Arg70 charged residues at the base of the TMP-binding cavity of *Sa*TMK .[10] We designed benzylidene phenyl acetamide-based derivatives. In some literature,[11] they were reported piperidinyl thymine's analogs for TMK target and also reported MIC IC_{50} values *SaTMK* 3.4 µM and p*henomena TMK* 156 µM and ligan showed interaction with amino acids Arg70, Ser97, Gln101 and Phe66 with pi-pi stacking. Although various scaffolds have been explored as potential TMK inhibitors for different bacteria, but not in specific *S. aureus*, a notable gap exists in identifying a specific scaffold for SaTMK. In this context, a study identified benzylidene phenylacetamide inhibitors as potential candidates for *SaTMK*, and an approach involved in silico high-throughput virtual screening, followed by molecular docking, molecular dynamics and in-vitro studies.

the selection of inhibitors, those are 2-(4-((3-nitrobenzylidene)amino)phenoxy)-N-phenylacetamide (**C$_1$**), N-(3-chlorophenyl)-2-(4-((4-

nitrobenzylidene)amino)phenoxy)acetamide(**C2**), 2-(4-((2,4-dichlorobenzylidene)amino)phenoxy)-N-(2,5-dimethylphenyl)acetamide(**C3**), N-(3-bromophenyl)-2-(4-((2,4-dichlorobenzylidene)amino)phenoxy)acetamide (**C4**), N-(3-chlorophenyl)-2-(4-((2,4-dichlorobenzylidene)amino)phenoxy)-N-(2,4,5-trichlorophenyl)acetamide (**C5**)and N-(3-chlorophenyl)-2-(4-((2,4-dichlorobenzylidene)amino)phenoxy)acetamide (**C6**)was shown high glide score, binding affinity, and compared with standard drug *ciprofloxacin* and we performed subsequent synthesis and in vitro studies. The Benzylidene Phenyl acetamide-based derivatives mentioned have been derived from various active moieties, as illustrated in (figure 2), each serving distinct therapeutic purposes across different diseases. For instance, benzylidene derivatives are employed in cancer treatment.[12] Phenoxy derivatives find application in anti-inflammatory and antibacterial medicine.[13] Phenyl acetamides are utilized in anti-filarial, anti-malarial, antifungal, and antimicrobial treatments.[14] These compounds exhibit versatility in their therapeutic potential, targeting various health conditions such as cancer, antiviral infections, filariasis, microbial infections, fungal infections, and inflammatory disorders. These Benzylidene Phenylacetamide-based derivatives can show promise in developing new antibiotics to combat *Staphylococcus aureus* infections, offering a potential solution to the challenges posed by antibiotic resistance.

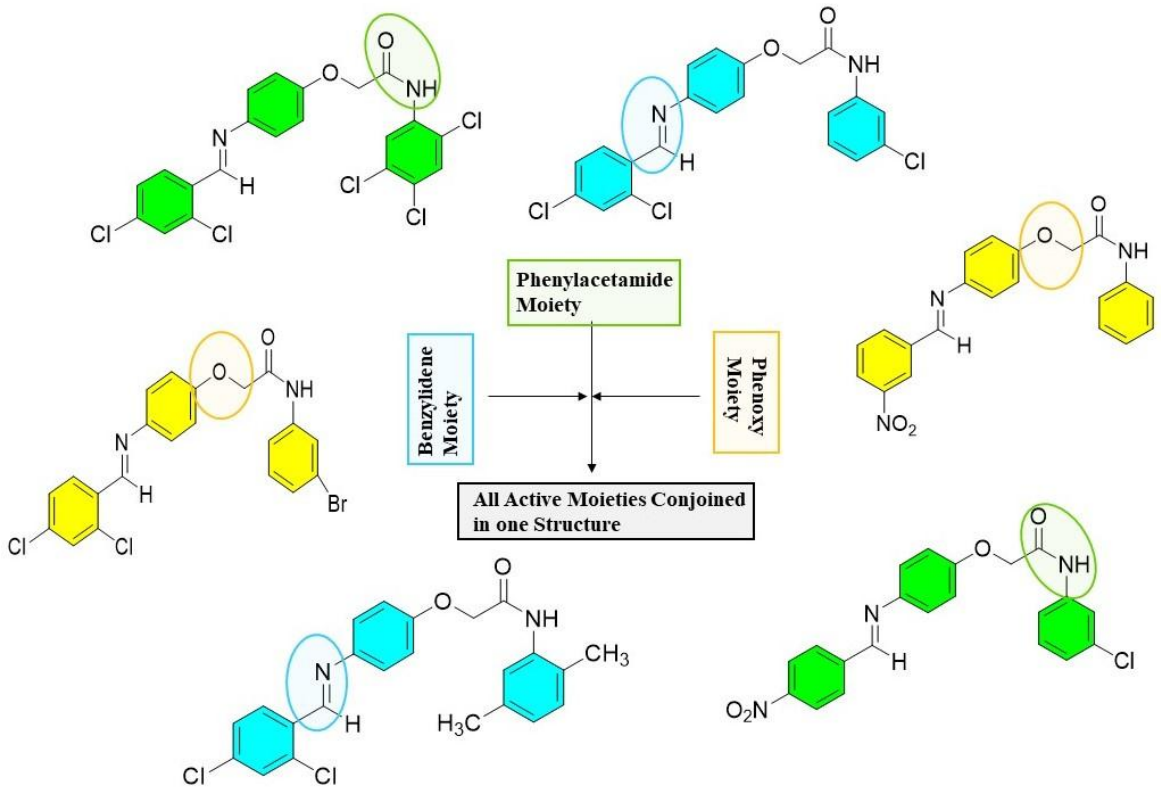


Figure 2 Incorporating pharmacophoric groups into derivatives of (4- (benzylidene amino) phenoxy)-N-phenylacetamide is part of the design process.

MATERIALS AND METHODS

Computational studies

Molecular docking

Molecular docking, a computer technology, has been employed to predict the binding mechanism and affinity of the ligands for the target. The docked conformers were adjusted based on the system's total energy.[15] The modeling effort focused on the X-ray crystal structure of *Staphylococcus aureus TMK* (pdb.4HLC, Resolution: 1.55 Å).[5] The protein preparation was carried out using the Schrödinger suite 2021-4 Wizard module,[16] which involved adding hydrogen and eliminating crystallographic water molecules.[17] Prime (Schrödinger suite 2021-4) accommodated missing side chains to minimize energy consumption and maintain an RMSD (root mean square deviation) of heavy atoms at 0.30; the OPLS3e forcefield was applied.[18] The active site was defined by a radius of ten around the bound ligand within a grid box, with the co-crystallized ligand positioned at the center.[19] Glide was employed for docking the six

synthesized ligands, prepared with LigPrep in extra-precision (XP) mode, with all other settings set to default. The optimal docked orientation for each ligand was determined based on Glide energy, score, and e-model values.

Binding free energy calculations using prim MM-GBSA

The prime Molecular Mechanics-Generalized Born Surface Area (MM-GBSA) approach, provided by Schrödinger suite 2021-4, was employed to calculate the binding free energy for each protein-ligand combination. Energy minimization was conducted using the OPLS3e force field coupled with the VSGB 2.0 solvation model.[20] This technique incorporates an optimal implicit solvation model for factors such as hydrogen bonding, self-contact interaction, and hydrophobic interactions, along with a physics-based correction.

Molecular dynamics simulations

We conducted molecular dynamics (MD) simulations using Schrödinger, suite 2021-4, to explore the nuclear binding behaviour and comprehend molecular interfaces of the top-ranked compound.[21] For the complex C_3/4HLC, the TIP4P water model with orthorhombic periodic boundaries and a 10-unit buffer zone between protein atoms and box edges was employed.[22] NaCl counter ions were introduced to neutralize the generated system at a 0.15 molar concentration. The plan was minimized using the OPLS4 force field adjustments. Long-range electrostatic interactions were calculated using the Ewald Smooth Particle Mesh method with a tolerance of 1e-09.[23] Short-range van der Waals and Coulomb interactions were estimated with a cutoff radius of 9.0. MD simulations of 100 nanoseconds were performed with a time step of 2 femtoseconds at 300 Kelvin and 1 bar pressure in an isothermal-isobaric ensemble (simulation of a system with constant number (N) and constant temperature (T), but variable pressure (P)). The Nose-Hoover chain thermostat and Martyna-Tobias-Klein barostat techniques were integrated at 100 and 200 picoseconds.[24] Multiple time-step methods were employed in the reference system propagator algorithm for bonded electrostatic forces, whether non-bonded, short-range, or long-range. Data was collected every 100 picoseconds, and trajectories were subsequently analyzed.

Synthesis part

Before use, the synthesized glassware underwent drying in a hot air oven. Solvent distillation and drying procedures were executed as required. The progression of reactions was tracked through thin-layer chromatography (TLC) using Merck-purchased plates of TLC silica gel 60 F_{254}. Isolated material yields are provided. Whenever applicable, purification utilized silica gel with particle sizes of 200-400 mesh and a pH of 7. Carbon ^{13}C NMR spectra were recorded on a Bruker 400 MHz instrument using deuterated chloroform ($CDCl_3$), while proton (^1H) NMR spectra were documented on a Bruker 400 MHz instrument. Chemical shifts are expressed in δ ppm and calibrated with $CDCl_3$ as an internal reference. Additionally, coupling constants (J) were provided in Hz wherever possible. Molecular weight predictions were conducted through Mass Spectrometric analyses using an LC instrument (Agilent 400 MHz series) equipped with an ESI source and linked with a mass spectrometer (SA/AD/INS/015 series). The instrument operated in positive ionization mode at Scan ES+ 1.01e5.

The General Protocol for the Synthesis of Compounds A_1-A_4.

~~The Schiff base reaction procedure for non-polar groups substituted benzaldehyde derivatives from the standard protocol.~~ ~~Specifically,~~ 1 gram of substituted benzaldehydes (10 mM) and 1.02 grams of p-amino phenol (10 mM) were stirred in absolute ethanol (20 mL) for 18 hours at 27°C[25]. The reaction progress was monitored using thin-layer chromatography (TLC) with ethyl acetate/hexane (3:7) solvent mixture, followed by drying at 27°C.The excess solvent was removed under vacuum and the obtained product is recrystallized with methanol. and the resulting crude product was stored at a low temperature. The obtained compounds A_1, A_2, A_3, and A_4 displayed in (figure 3) were used in the subsequent step without further purification.

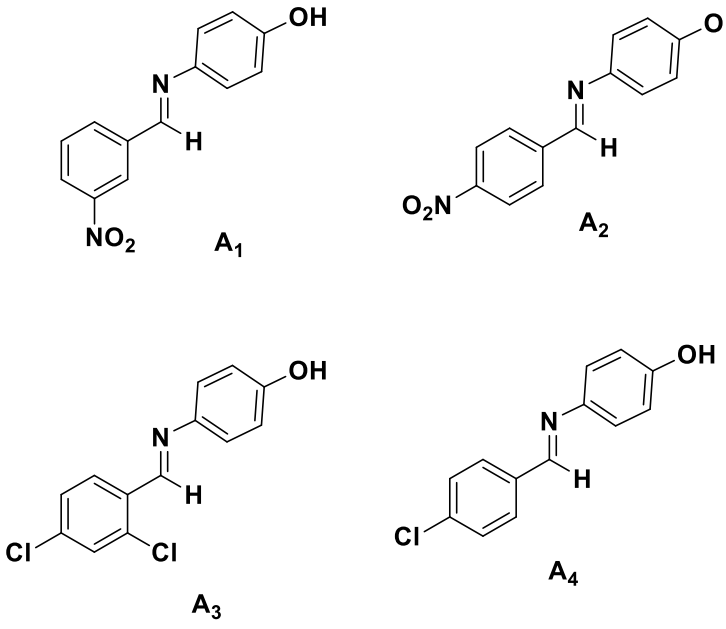


Figure 3. Synthesis of 4-(Benzylidene amino) phenyl moiety compounds A_1-A_4

The General Synthetic Procedure of Compounds B_1-B_5

Substituted anilines underwent acetylation by utilizing chloroacetyl chloride with anhydrous K_2CO_3 as a base and dichloromethane (DCM) as the solvent. In this process, a mixture containing substituted anilines (0.9 g, 1 equiv.), K_2CO_3 (2.00 g, 1.5 equiv.) in DCM (25 mL) and chloroacetyl chloride (0.7 mL, 1 equiv.) were -----. The chloroacetyl chloride was added drop-wise with stirring at 0°C.[26,27] The reaction mixture was stirred for 4 hours at 27°C, and thin-layer chromatography (TLC) with ethyl acetate/hexane (2:8) as eluent was employed to monitor the reaction progress. Upon completion, the excess solvent was removed under a vacuum, and the resulting solid was mixed with 25 mL of cold water. The obtained solid was washed twice with water and subsequently dried. The obtained intermediates B_1, B_2, B_3, B_4, and B_5 displayed in (figure 4) were used in the following step without additional purification.

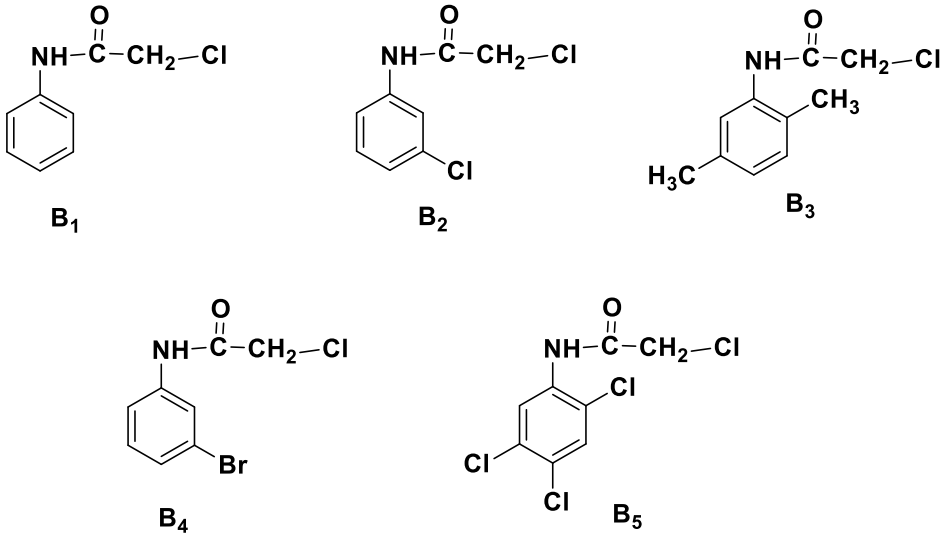


Figure 4. Synthesis of N-Phenylacetamide moiety compounds B_1-B_5

General Synthetic Procedure of compounds C_1-C_6 (4- (Benzylidene amino) phenoxy) -N-phenylacetamide derivatives.

A solution of 4-(benzylidene amino) phenol (1.1 g, 1 equiv.) was ~~prepared,~~ and anhydrous K_2CO_3 (2.31 g, 3 equiv.) was added to the mixture. The solution underwent stirring at 40°C for 2 hours. Subsequently, 2-chloro-N-Phenylacetamide (0.94 g, 1 equiv.) was introduced to the above mixture, and stirring continued at 40°C for 24 hours. The progression of the reaction was monitored using thin-layer chromatography (TLC) .26,27 After the completion of the reaction, excess acetone was removed under vacuum, and the resulting solid

was washed twice with water and dried. Column chromatography was then employed to purify the title molecules C_1–C_6 displayed in (figure 5), using ethyl acetate/hexane (2:8) as the eluent.

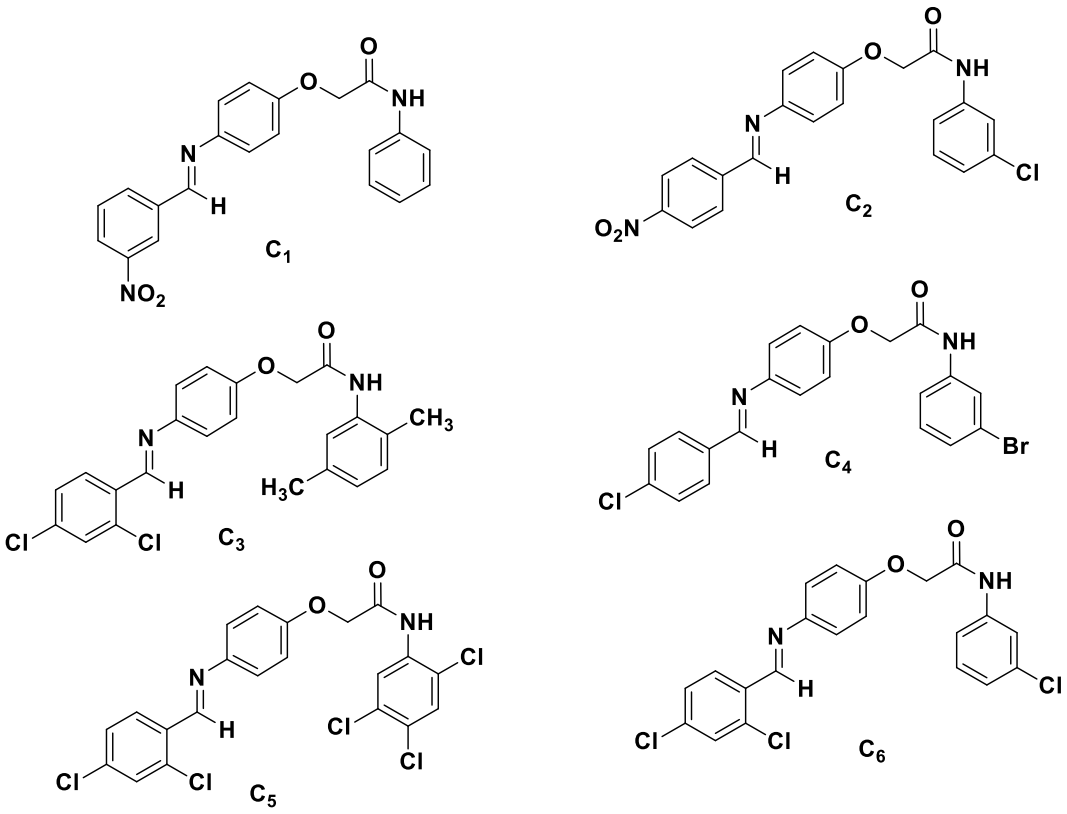


Figure 5. Synthesis of (4-(Benzylidene amino) phenoxy)-N-Phenylacetamide moiety compounds C_1-C_6

IN VITRO SCREENING

Minimum Inhibitory Concentration (MIC) Determination

The minimum inhibitory concentration (MIC) of the compounds C_1-C_6 was assessed against Gram-positive strains of *S. aureus* (NCIM 5021, NCIM 5022), clinical *MRSA* strains (ATCC 43300), *Staphylococcus epidermidis* (NCIM 2493), *Pseudomonas aeruginosa* (NCIM 2036), and *Escherichia coli* (NCIM 2065) following the Clinical Laboratories Standard Institute (CLSI) guidelines from 2017.[28] Bacterial cultures were diluted at a ratio of 1:1000 in nutrient broth to achieve a turbidity of McFarland 0.5. The MIC was determined using the micro-broth dilution method in Mueller-Hinton medium (Hi-media). *Ciprofloxacin* was the positive control, and sterile dimethyl sulfoxide (DMSO) was used as the negative control. Before the study, compounds C_1-C_6 and the positive control were dissolved in pure DMSO.

In each 96-well plate, 100 µL of bacterial culture was combined with 50 µL of the title compounds, and a serial dilution of the mixture was conducted. Following bacterial inoculation, the plates were incubated at 37°C for 20–24 hours, except for *P. aeruginosa,* where the incubation was extended to 24–28 hours at 37°C. Bacterial inoculums were adjusted to 1×10^6 CFU/mL. The absorbance was measured at a wavelength of 600 nm using Tecan-i-control, 1.7.1.12. The MIC data obtained are expressed in micrograms per milliliter (µg/mL).

Minimum Bactericidal Concentration (MBC) Determination

The minimum bactericidal concentration (MBC) of a chemical compound, drug, or antibiotic refers to the lowest concentration capable of killing bacterial cells within a defined timeframe and under specific conditions. The MBC determination for the title compounds (C_1-C_6) was conducted against a selected panel of pathogenic bacteria using a previously reported method.[29] Three consecutive concentrations above the minimum inhibitory concentration (MIC) were employed, with 20 µL of bacterial aliquots sub-cultured onto nutrient agar plates. The agar plates were incubated for 24 hours at 37°C, followed by colony counting to determine the initial inoculum. The colony-forming units per milliliter (CFU/mL) were then calculated. The concentration at which a > 99% reduction or inhibition of bacterial growth occurred (3 log10 reduction CFU/mL) was considered the MBC. The obtained MBC values and the MBC/MIC ratio.

Time-Kill Analysis

Time-kill kinetics is a study designed to evaluate the bactericidal or bacteriostatic properties of antibacterial agents over a specified duration, and it was conducted following a standard protocol provided by CLSI.[30] Sample concentrations equivalent to 1× MIC and 0.5× MIC were prepared with bacterial culture and then incubated at 37°C. At regular intervals of 0, 2, 4, 6, 8, 12, and 24 hours, a 50 µL aliquot of the culture was inoculated onto a solidified agar plate, followed by a 24-hour incubation at 37°C. In this study, *ciprofloxacin* and DMSO were positive and negative controls, respectively. Nutrient broth and agar were also cultured separately on the solidified agar plate and incubated to mitigate any potential bias in the results. The colony-forming units (CFU) were determined based on the hardened agar plate observations. A time-kill graph plotting log CFU/mL against time was generated. The obtained Time kill values.

RESULTS AND DISCUSSION

Binding free energy calculations and molecular docking

Schrodinger Suite 2021-4 employs TMK (PDB-4HLC) to validate docking studies through ligand-based virtual screening techniques. The conformational orientation of the bound ligands accurately matches the co-crystal, with a Root Mean Square Deviation (RMSD) of 1.01 Å achieved using the docking protocol. This docking approach utilizes a virtual screening strategy to eliminate functional groups interacting with ligands, adhering to Lipinski's rule. The XP-docking results regarding glide score, emodel, evdw, ecoul, and energy are expressed.

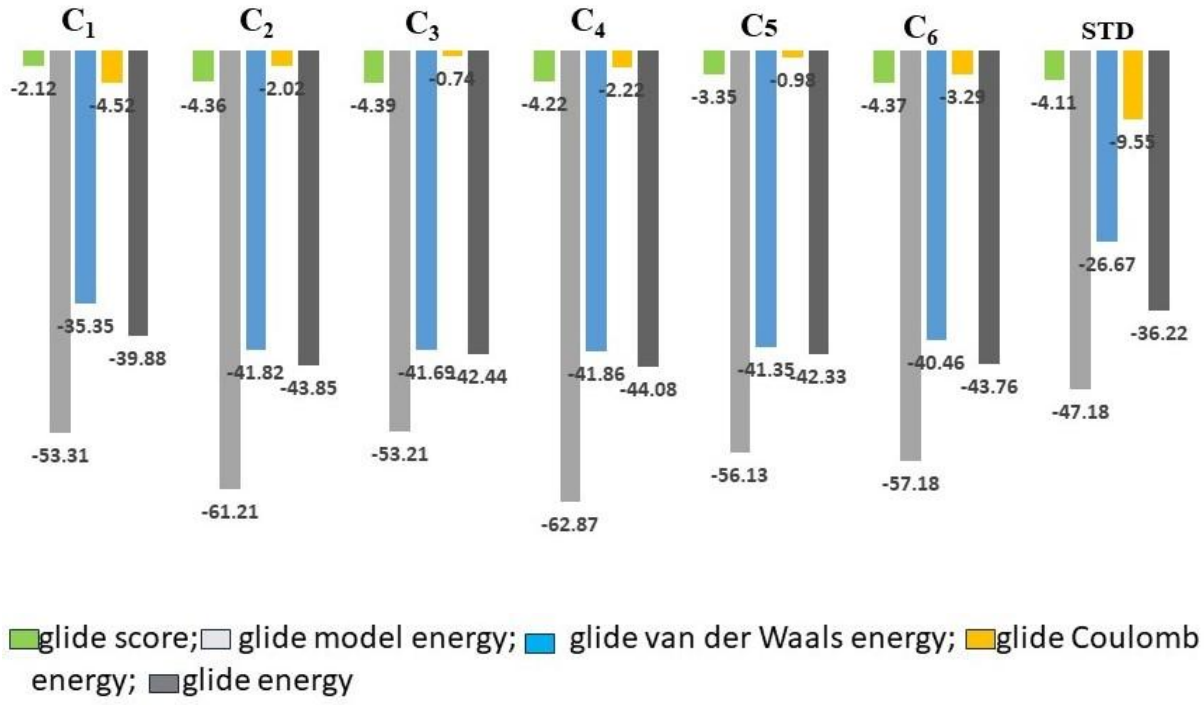


Figure 6. The XP-docking score of compounds C_1-C_6 in the catalytic pocket of (PDB:4HLC)thymidylate kinase (kcal/mol).

The docking outcomes presented in (supplementary table 1) reveal that each ligand establishes a minimum of one hydrogen bond with amino acids, accompanied by favourable glide scores range from -4.39 to -2.12 kcal/mol. In the context of XP-docking, Compounds C_3, and C_6 displayed notably elevated glide scores, -4.39 and -4.37 kcal/mol, respectively (figure 6). After docking, the minimized binding free energies (ΔG_{Bind}) for the top-scoring poses of the identified hits exhibited a substantial increase, ranging from -101.54 to -53.62 kcal/mol. All data presented in (supplementary table 2) illustrates a noteworthy range of Van der Waals energy (ΔG_{VdW}) spanning from -60.51 to -33.03 kcal/mol, complemented by a moderately favored hydrophobic component (ΔG_{Lipo}) varying from -35.89 to -17.39 kcal/mol, contributing to the overall favorable total binding energy. Compounds C_2 and C_4 exhibited

outstanding ΔG_{bind} scores of -98.05 and -101.54 kcal/mol, respectively.) Furthermore, riming compounds demonstrated the highest binding affinity, recording -78.27 kcal/mol for C_5 and -76.93 kcal/mol for C_3, and one more -65.81 kcal/mol for C_6, as determined by the critical free energy calculation using the MMGB-SA method (figure 7).

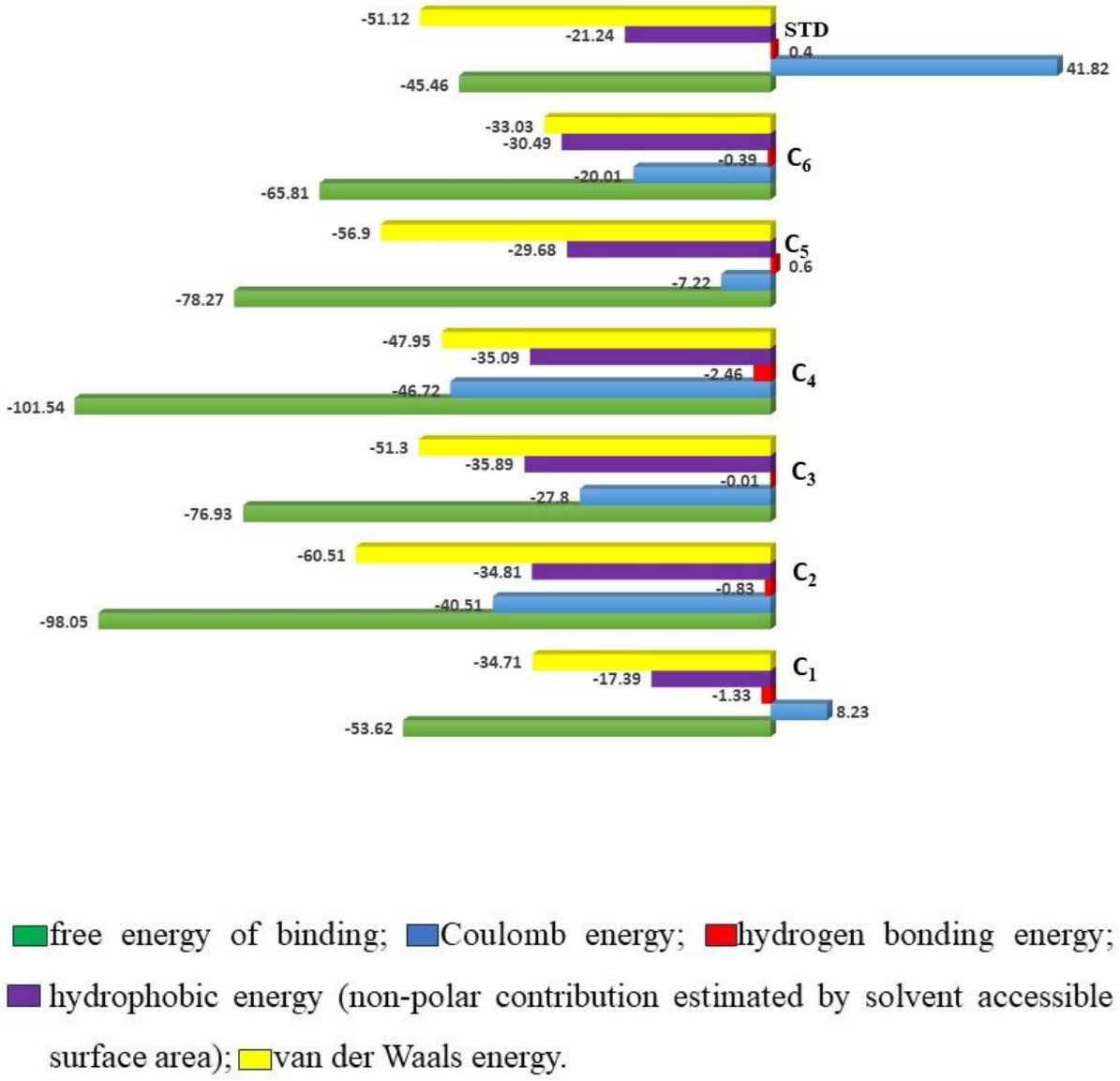


Figure 7. Contribution of binding free energy (MM-GBSA) (kcal/mol) between compoundsC_1-C_6 (PDB:4HLC) thymidylate kinase complexes.

As illustrated in figure 8, the C_1 molecule engages in interactions with Met57 amino acid, forming a hydrogen bond between the oxygen group and Asp56 forms a hydrogen bond with carboxylic group.C_2 molecule Arg70 shows interaction with phenoxy group with hydrogen bond ,Phe66 shows interaction with benzene ring with pi-pi stacking ,Arg72 shows interaction

with aromatic ring with pi-cation,Arg105shows interaction with oxygen group with salt bridge.C_3 molecule Phe66 shows interaction with benzaldehyde ring and phenol ring with pi-pi stacking ,Arg92 shows interaction with aromatic ring with pi-cation.C_4 molecules Phe66 shows interaction with benzene ring with pi-pi stacking ,Arg48 shows interaction with bromine with halogen bond .C_5 molecule Phe66 shows interaction with benzene ring with pi-pi stacking ,Arg96 shows interaction with benzene ring with pi-cation ,C_6, molecule Arg70 shows interaction with phenoxy group with hydrogen bond ,Arg48 shows interaction with chlorine with halogen bond ,Arg92 shows interaction with benzene ring with pi-cation ,Phe66 shows interaction with benzene ring with pi-pi stacking .

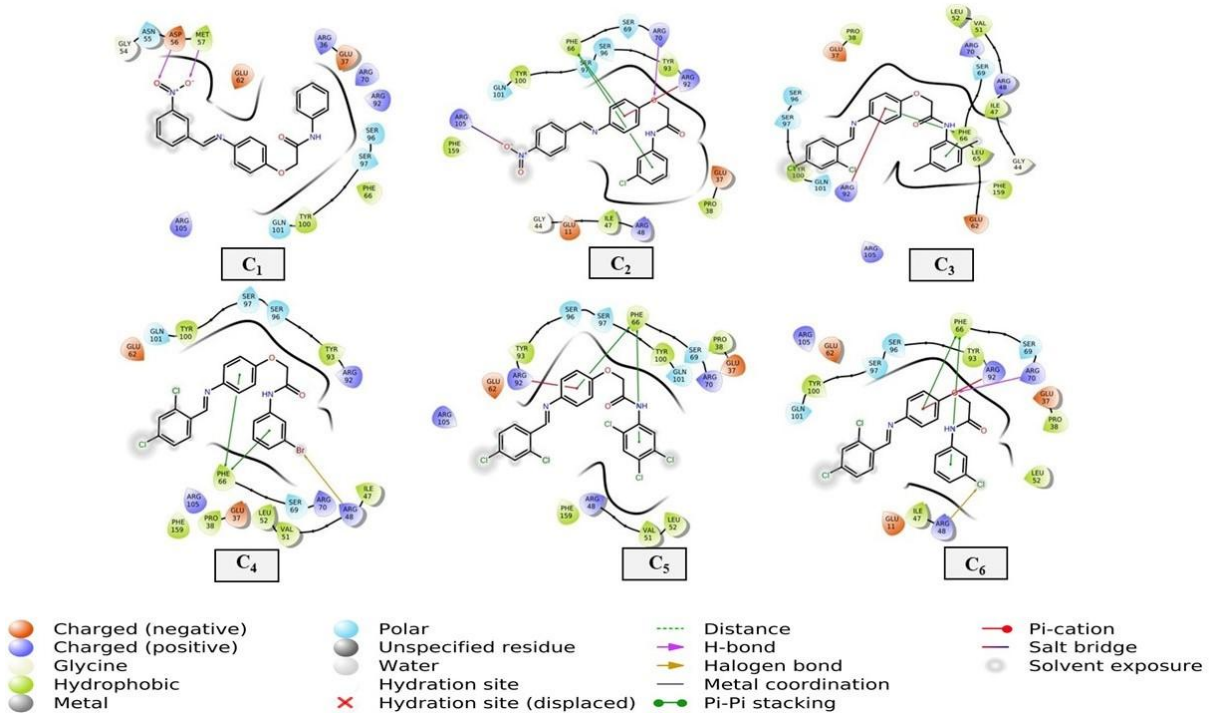


Figure 8. 2D interaction diagrams of the Six ligands c1-c6 in the thymidylate kinase catalytic pocket (PDB:4HLC).

We have taken ciprofloxacin as a standard drug, illustrating the 2D interactions of ciprofloxacin and all-molecule hits, in ciprofloxacin Gln101 shows interaction with a carboxylic group with hydrogen bond, Glu37 shows interaction with hydrogen group with hydrogen bond, Arg105 shows interaction with the carboxylic group and oxygen with hydrogen bond and salt bridge. here we have taken ciprofloxacin compression for all criteria like glide score binding affinity and interactions with amino acids. Here C_3, C_6, and

ciprofloxacin showed a gliding score of -4.39, -4.37, and -4.11 kcal/mol, respectively and C_3, C_6, and ciprofloxacin an impressive binding affinity of -76.93, -65.81 and -45.46 kcal/mol. Respectively. Here **C_3** ligand has shown an impressive glide score and binding affinity score compared with the standard drug ciprofloxacin as shown in (figure 9).

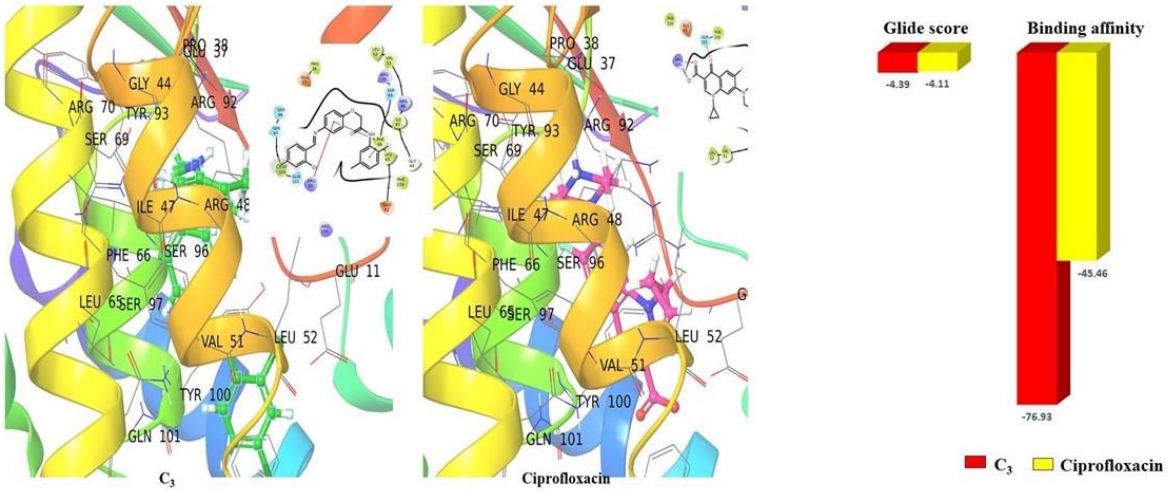


Figure 9. 2D and 3D interaction diagrams of the C_3 ligand and Ciprofloxacin in the thymidylate kinase catalytic pocket (PDB:4HLC).

The hydrogen bond, pi-pi stacking interactions shown between designed molecules with amino acid residues. The selection of molecules for further investigation was based on a comprehensive evaluation of both docking glide scores and binding affinity, especially in comparison to C_3 with standard drug (ciprofloxacin), which did not exhibit consistent docking and ΔG_{bind} stability~~. Notably, C_3 maintained a steady gliding score and binding affinity.~~ Consequently, we conducted an in-depth investigation through MD simulation studies focusing on C_3.

MD simulation study

The docked pose of the ligand 2-(4-((2,5-dichlorobenzylidene) amino) phenoxy)-N-(2,5-dimethylphenyl) acetamide, C_3/4HLC, underwent a 100 ns molecular dynamic simulation. The study analyzed results based on various parameters, including root mean square deviations (RMSD), root mean square fluctuations (RMSF), protein-ligand interaction fractions, protein-ligand contacts timeline, and protein-ligand contacts illustrated through a 2D diagram.

Specifically, observations were made on the Cα atom of the ligand fitting onto the protein (prot). In the RMSD analysis, the Cα atom (lig) fit prot demonstrated stability range from 1.15 to 1.40 Å, with specific values of 0.80 to 1.50 Å. Notably, the Cα atom of the ligand-maintained stability throughout the 65 ns, with a consistent period of stability from 20 to 75 ns and 75 to 100 ns. During the 25 ns interval, moderate fluctuations were observed, spanning the entire 100 ns duration. Similarly, the (lig) fit prot for the ligand exhibited stability during the first 65 ns, with consistent periods of stability from 20 to 75 ns out of 100 ns. Moderate fluctuations were evident at 75ns, covering the entire 100 ns as depicted in (figure 10, a).

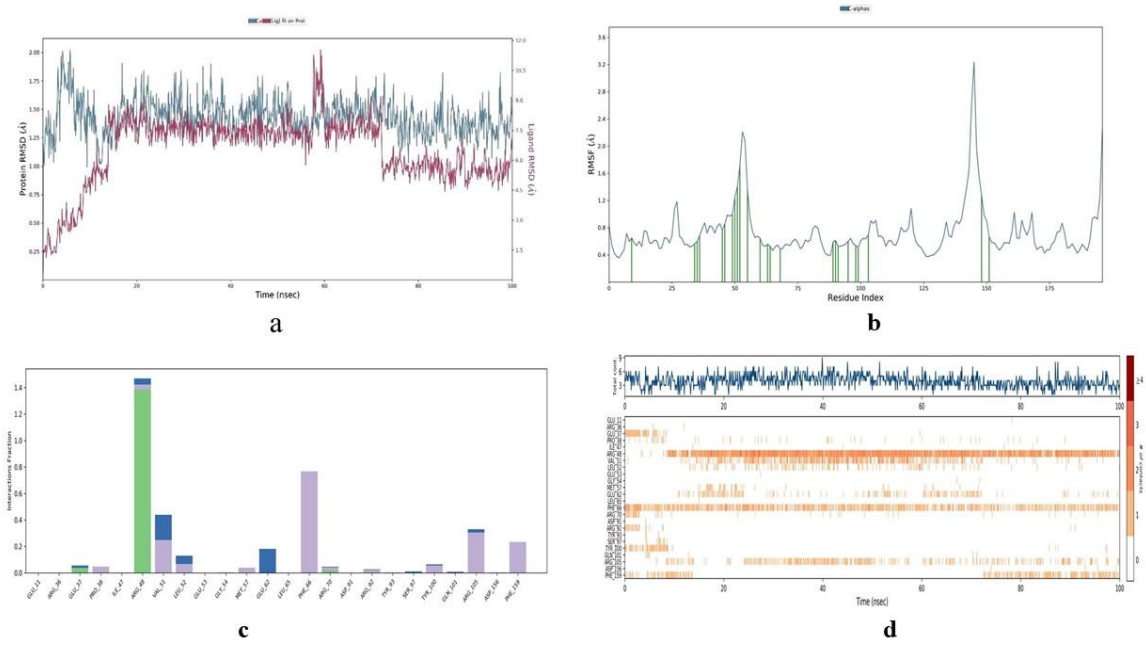


Figure 10. **(a) RMSD (b) RMSF (c) Protein-Ligand interactions (d) Protein-Ligand interactions for C_3/4HLC complex**

The RMSF analysis of the Cα atom revealed fluctuations ranging from 0.5 to 2.3 Å, as depicted in (figure 10, b), maintaining consistency throughout the simulation. Notably, ligands exhibited specific variations in their interactions with amino acids, with minimum and maximum fluctuations observed between 30 to 105 ns, and 150 ns. During these specific intervals, amino acids demonstrated changes of 0.5 to 2.3 Å, and 0.6 to 1.6 Å, respectively.

In (Figure 10, c), amino acids are observed to simultaneously engage in interactions involving water bridges, hydrogen bonds, ionic bonds, and hydrophobic interactions. Multifaceted exchanges are also depicted in the illustration. Specifically, in the ligand C_3 protein-ligand

contacts, amino acids of the protein initiate interactions with water bridges, including Arg48, Glu37, Val51, Leu52, Glu62, Ser97, Tyr100, Glu101, and Arg105, with water bridge interactions being maintained at 0.22% out of a total of 1.5%. Hydrophobic interactions with Val51, Leu52, Met57, Phe66, Arg70, Arg48, Arg92, Tyr100, Arg105, and Phe159 constitute 0.8% of the total interactions of 1.5%. Hydrogen bond interactions with Arg70, Arg48, and Glu37 amino acids contribute to interactions at a rate of 1.3% out of 1.5%. Additionally, multifuel interactions involving amino acids, Glu37, Arg48, Val51, Leu52, Arg70, Arg92, Ser97, Tyr100 and Arg105 constitute 1.43% of the total interactions of 1.5%.

In (figure 10, d) highlights amino acids, namely Arg48, phe66, and Arg105, that consistently maintained contact with the ligand. Arg48 exhibited continuous contact with the ligand at 10 to 100 ns. Arg105, on the other hand, sustained constant contact with the ligand throughout the entire 10 to 100 ns duration. Additionally, Phe66 maintained continuous contact with the ligand from 0 to 100 ns. These protein-ligand contacts were observed consistently over the whole 100 ns of simulations.

The 2D diagram illustrating protein-ligand connections is presented in (figure 11). Phe66 consistently maintained continuous contact with the ligand aromatic ring through pi-pi interactions, with the bond stability recorded at 16%. Simultaneously, Arg48 established connections with the ligand acetamide group through hydrogen bonds, maintaining stability at 138%. Glu62 and Val51 have shown the contacts with benzylidene group with hydrogen bond at 18%. Phe159 showed interaction with the benzene ring with pi-pi-stacking with 14%. Arg105 has shown interaction with benzene ring with pi-cation bond with 30%, throughout the specific studies, in an overall assessment, the ligand C_3 has shown the interactions with design amino acids arg48, has shown the interaction with active moiety acetamide and Glu62, Val51 have shown the interaction with benzylidene active moiety which we design the ligand for specific target that's the reason the ligand would be demonstrated promising activity, suggesting its potential for developing new antimicrobial agents.

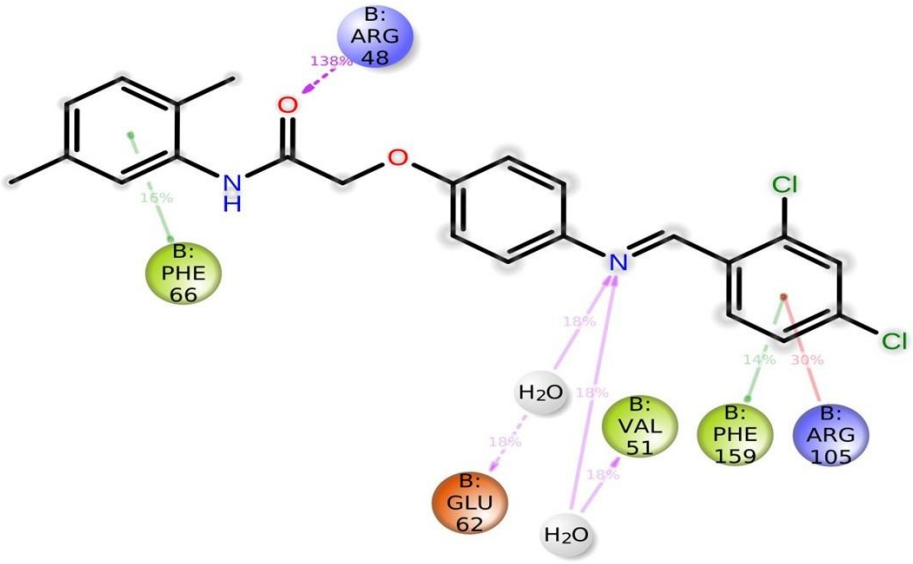
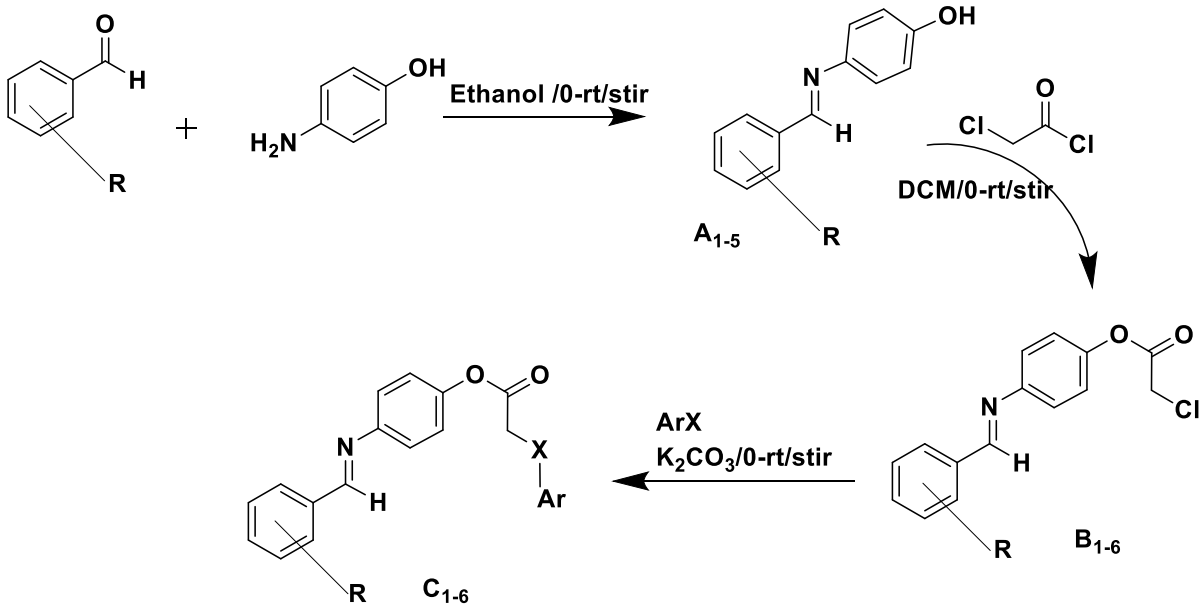


Figure 11. 2D diagram for C_3/4HLC complex

SYNTHESIS PART

The synthesis of derivatives C_1-C_6, specifically (4-(benzylidene amino) phenoxy) -n-phenylacetamide, was conducted following the procedures outlined in Scheme 1



X=NH,NHNH
Ar=Benzothiozole,4-Methylbenzothiozole,4-Chlorobenzothiozole,4-ethoxybenzothiozole, 4-nitrobenzothiozole,Aniline.
R=4-OCH_3,4-NO_2,4-CN,4-Cl,2,4-di-cl,4-Br.

Scheme 1 synthesis of (4-(benzylidene amino) phenoxy) -N-phenylacetamide derivatives C_1-C_6.

In the initial step the compounds A_1-A_4 were prepared by mixing benzaldehyde and aminophenol in absolute ethanol at room temperature~~, following the Schiff base procedure~~. The intermediate compounds (B_1-B_5) were obtained reacting an appropriate substituted aniline with chloroacetyl chloride in dichloromethane at 0°C, in the presence of anhydrous potassium carbonate. The title compounds C_1-C_6 were synthesized by reacting of 4-(benzylidene amino) phenol (A1-A4) and 2-chloro-N-phenylacetamide (B1-B5)in acetone and K_2CO_3 at 40°C for 24 hours (Figure 11). Following the procedure outlined in Scheme 1, we successfully prepared (E)-2-(2-((2,4-dichloro benzylidene) amino) phenoxy)-N-(2,5-dimethyl phenyl) acetamide in (Figure 11) using the starting material 2-((2,4-dichloro benzylidene) amino) phenol and the intermediate 2-chloro-N-(2,5-dimethyl phenyl) acetamide**.**

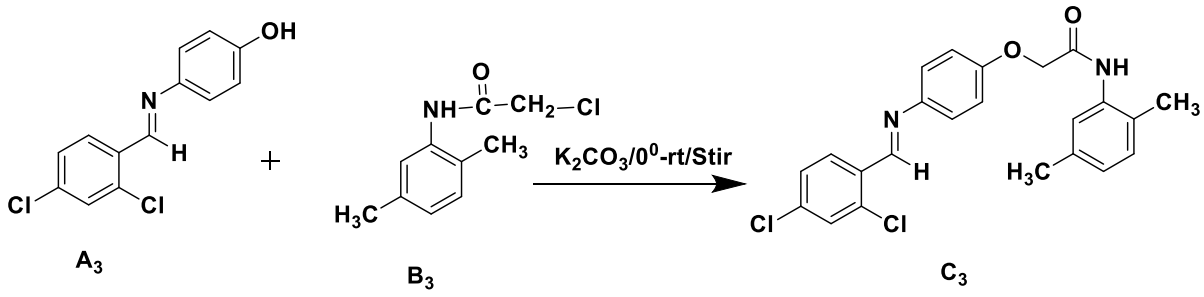


Figure 11. synthesis of (E)-2-(2-((2,4-dichloro benzylidene) amino) phenoxy)-N-(2,5-dimethyl phenyl) acetamide compound (C_3)

In Figure 11, we present the compound denoted as (C_3), for which we conducted a comprehensive characterization involving mass spectrometry, Nuclear Magnetic Resonance (proton ^{1}H NMR), and ^{13}C-NMR. Compound (C_3) was purified using column chromatography with an ethyl acetate/hexane mixture (2:8 ratio) as the eluent. In the Fourier-transform infrared (FT-IR) Spectrum, characteristic absorption bands were observed at wavenumbers (KBr, cm-1) of 3357 (-NH-), 1689 (>C=O), 1629 (>C=N), 1542 (Ar-C=C-), 1513, 1349 (DI-Cl), 1062, 1119 (C-O-C), and 851 (p-substituted benzene) (supplementary data 2). For mass spectrometry characterization data present in (supplementary data 3), the molecular weight of compound (C_3) was determined to be 427.33 g/mol, with a molecular formula of $C_{23}H_{20}Cl_2N_2O_2$. The mass calculation (m/z) was 428.8 (M^++H) using the SA/AD/INS/015 instrument. Structural characterization of the synthesized compound (C_3) was carried out using proton-nuclear

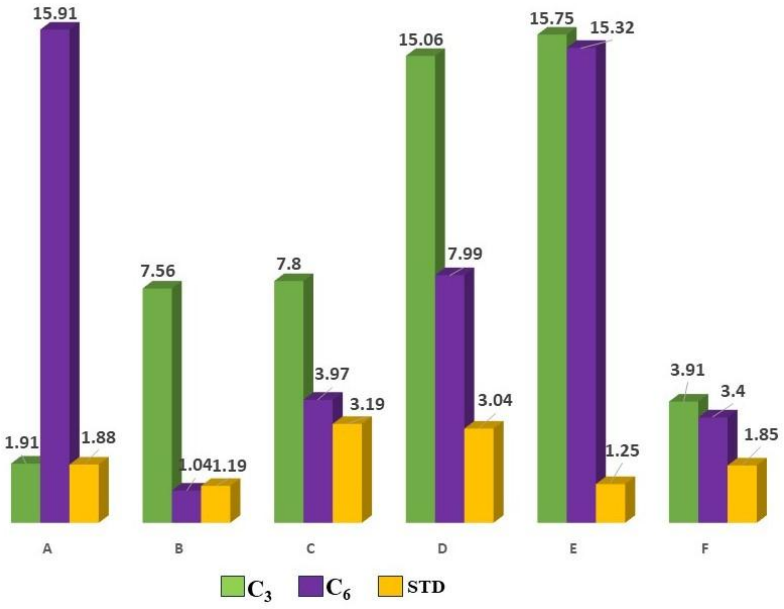
magnetic resonance ^{1}H-NMR and ^{13}C-NMR (supplementary data 4). The ^{1}HNMR prediction protocol revealed specific proton signals, including -NH- and -N=CH- proton signals for phenylacetamide and benzylidene derivatives have been observed in the region of from δ 9.0 and 8.86ppm. the peaks approved in the region from δ 4.76,2.31 and 2.01 ppm were attributed to the characteristic -CH_2-, -CH_3-, and -CH_3- singlet of the C_3 compound. In the ^{13}C-NMR spectra, the carbonyl groups of title compounds appeared as singlet signals in the region δ 166.65 ppm in contrast to the aromatic carbons that appeared in the expected region in compound C_3 one (>C=O) peaks that appeared at δ 166.65 ppm whereas, three signals observed at δ 69.93,21.08 and 17.13 ppm are ascribed to carbons of -CH_2-, -CH_3-, and -CH_3-of the compound. the mass spectra of the compound in conformity with their respective molecular formula (supplementary data1).

IN-VITRO

Minimum Inhibitory Concentration (MIC) Determination

The susceptibility of title compounds was assessed through microbial screening using the micro broth dilution method, adhering to the Clinical and Laboratory Standards Institute (CLSI) 2017 guidelines.[28] Antibacterial screening involved a chosen panel of bacteria, including Gram-positive strains *S. aureus* (NCIM 5021, NCIM 5022), clinical *MRSA* strains (ATCC 43300), *Staphylococcus epidermidis* (NCIM 2493), as well as Gram-negative strains *Pseudomonas aeruginosa* (NCIM 2036) and *Escherichia coli* (NCIM 2065). The test concentration range was 250 to 1.95 µg/mL. ~~here, we have taken two compounds for inhibitory assay because these compounds have shown good binding affinity.~~ In the docking studies, two tested compounds (C_3 and C_6) exhibited significant inhibitory activity against the selected bacterial strains, as indicated by noteworthy inhibitory values (supplementary table). Compounds C_3 and C_6 demonstrated notable inhibitory activity against *S. aureus* (NCIM 5021) and *MRSA* (ATCC 43300). Compound C_3 exhibited varied activity against gram-positive bacteria with MIC values of 1.91 µg/mL (S. aureus, NCIM 5021) and 3.91 µg/mL (MRSA, ATCC 43300). Meanwhile, compound C_6 displayed varied activity against both gram-positive and gram-negative bacteria, with MIC values of 1.04 µg/mL *S. aureus (NCIM 5022), 3.97 µg/mL Escherichia coli* (NCIM 2065), and 3.40 µg/mL *Pseudomonas aeruginosa,* (NCIM 2036).In comparison with the standard compound *ciprofloxacin*, compounds C_3 and C_6 exhibited ~~competitive inhibitory~~ activity against *S. aureus* (NCIM 5021, 5022), *Escherichia coli* (NCIM 2065), and *MRSA*

(ATCC 43300), with MIC values of 1.88 µg/mL, 1.19 µg/mL, 3.19 µg/mL, and 1.85 µg/mL, respectively (figure 11).



(**A**)*S. aureus* (NCIM 5021), (**B**) *S. aureus* (NCIM 5022), (**C**) *Escherichia coli* (NCIM 2065) (**D**) *Staphylococcus epidermidis* (NCIM 2493), (**E**) *Pseudomonas aeruginosa* (NCIM 2036), (**F**) *MRSA* (ATCC 43300).

Figure 11. The minimum inhibitory concentration **(µM)** of synthesized compounds C_3 and C_6 against the selected bacterial strains.

Minimum Bactericidal Concentration (MBC)

In determining the minimum bactericidal concentration (MBC) for test compounds, C_3 and C_6 followed the CLSI guidelines 2017. MBC represents the lowest antibiotic concentration necessary to kill bacteria or achieve >99% inhibition of bacterial growth (figure 10 a). The MBC/MIC ratio provides insights into the antibiotic's profile, distinguishing between bactericidal and bacteriostatic activities. An MBC/MIC ratio less than 2 suggests bactericidal activity, while a ratio exceeding 4 indicates bacteriostatic activity. The MBC results for tested compounds, including C_3 and C_6, demonstrated promising activity, as detailed in the supplementary Table. Specifically, compound C_3 exhibited bactericidal activity against S. aureus (NCIM 5021) (MBC/MIC: 2) and MRSA (ATCC 43300) (MBC/MIC: 2). Compound C_6 demonstrated bactericidal activity against S. aureus (NCIM 5022) (MBC/MIC: 2), MRSA (ATCC 43300) (MBC/MIC: 4), and Escherichia coli (NCIM 2065) (MBC/MIC: 3), shown in

the (figure 12, b). The inhibitory activity of C_3 and C_6 was compared with the standard drug ciprofloxacin, further highlighting their potential as effective antimicrobial agents.

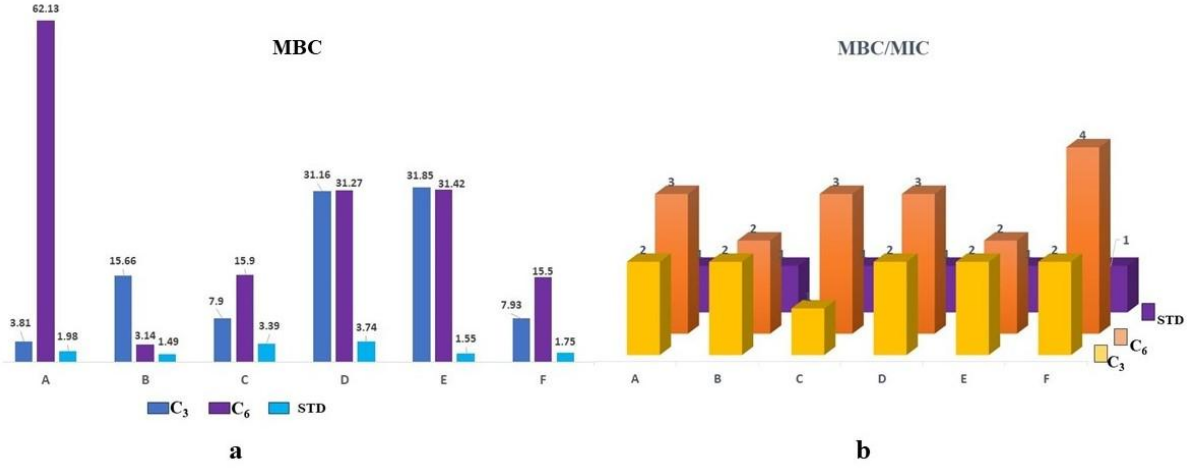


Figure 12. (a) The minimum bactericidal concentration (MBC) and (b) MBC/MIC ratio of title molecules C_3 and C_6 against selected bacterial strains.

(A) *S. aureus* (NCIM 5021), (B) *S. aureus* (NCIM 5022), (C) *Escherichia coli* (NCIM 2065) (D) *Staphylococcus epidermidis* (NCIM 2493), (E) *Pseudomonas aeruginosa* (NCIM 2036), (F) *MRSA* (ATCC 43300).

Time kill study

Compounds C3 and C6 have demonstrated promising Minimum Inhibitory Concentration (MIC) and Minimum Bactericidal Concentration (MBC) values against Gram-positive and Gram-negative organisms. Consequently, these compounds are being considered for further antibacterial evaluation. A time-kill study assessed the bactericidal properties of compound C3 against S. aureus (NCIM 5021). In this study, S. aureus bacteria were serially diluted to achieve a concentration of -105 CFU/ml and then treated with the test compound ciprofloxacin (used as a positive control) at concentrations of 0.5 and 1 MIC. The culture was incubated at 37°C, and 50 µL samples were collected and sub-cultured on nutrient agar at regular intervals of 0, 2, 4, 6, 8, 12, and 24 hours, respectively (Figure 12). After the incubation period, CFU (colony-forming units) were calculated, and a graph was plotted to illustrate the time-kill kinetics, with CFU/mL on the ordinate and time on the abscissa. The tested compounds exhibited significant bactericidal activity against the selected bacteria compared to untreated bacteria and those treated with ciprofloxacin.

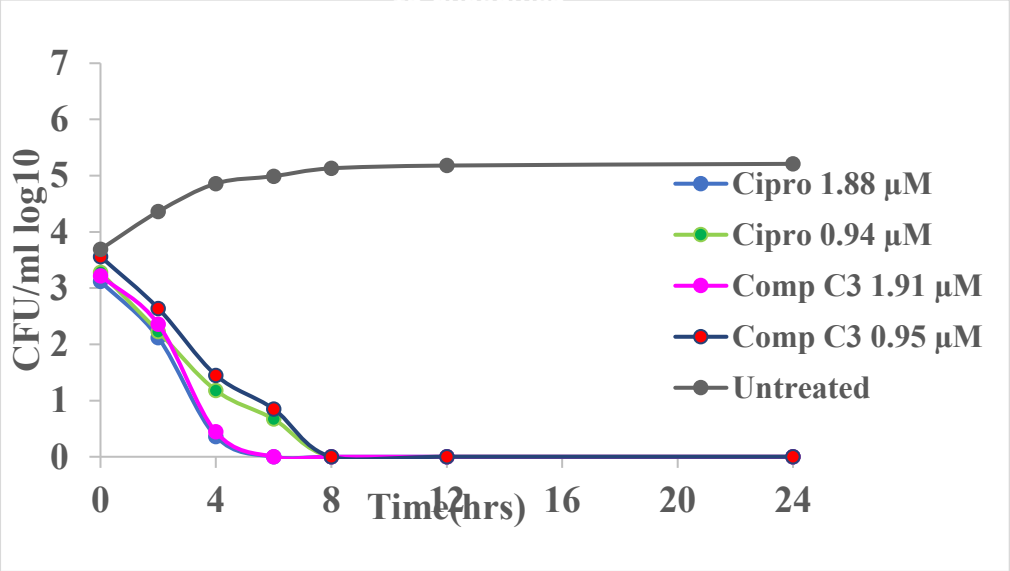


Figure 12 displays the time-kill plot depicting the impact of compound C_3 on Staphylococcus aureus (NCIM 5021).

This graph illustrates the changes in bacterial viability over time, offering insights into the bactericidal activity of compound C_3 against the specified strain of Staphylococcus aureus.

Conclusion

Antimicrobial resistance poses a significant challenge to public health, particularly with the widespread resistance observed in Staphylococcus aureus bacteria. According to statistical analysis, 1.27 million people succumbed to antibacterial resistance in 2019. The current study focuses on (4- (benzylidene amino) phenoxy) -n-phenylacetamide derivatives designed to target the thymidylate kinase enzyme in Staphylococcus aureus bacteria, employing XP-docking, MM-GBSA, and molecular dynamics.

Promising outcomes were observed, particularly for compound C_1, which exhibited a favorable glide score of -3.27 kcal/mol in XP-docking. The MM-GBSA analysis revealed significant binding affinity (Δ bind) at -65.80 kcal/mol, along with substantial contributions from ΔVdW (-55.10 kcal/mol) and ΔLipo (-28.55 kcal/mol). Molecular dynamics simulations further demonstrated continuous protein-ligand contacts with amino acid residues Arg36, Arg48, and Phe66.

In vitro results proved pivotal in identifying the antibacterial potential of these derivatives, with impressive MIC (1.91 µM) and MBC (3.81 µM) values. Based on these findings, it is suggested

that these derivatives can inhibit the thymidylate kinase enzyme, showcasing their potential as antibacterial agents in the future.

In conclusion, the performance of C_1 demonstrated favourable outcomes with a glide score of -3.27 kcal/mol in XP-docking. Notably, key parameters such as ΔBind (-65.80 kcal/mol), ΔVdW (-55.10 kcal/mol), and ΔLipo (-28.55 kcal/mol) obtained from (MM-GBSA) and during molecular dynamics (MD) simulations, targeted amino acids Arg36, Arg48, and Phe66 maintained the contacts with ligand. Then Minimum Inhibitory Concentration (MIC) against Staphylococcus aureus (NCIM) was measured at 1.91 μM, while MRSA (ATCC43300) exhibited a MIC of 3.91 μM. Based on these encouraging findings, these derivatives are anticipated to be potential future inhibitors of the *SATMK* enzyme, suggesting their potential role as antibacterial agents.

REFERENCE

1. Penchovsky R, Traykovska M. Designing drugs that overcome antibacterial resistance: where do we stand and what should we do? Expert opinion on drug discovery. 2015 Jun 3;10(6):631-50.
2. Yoshikawa TT, Bradley SF. Staphylococcus aureus infections and antibiotic resistance in older adults. Clinical infectious diseases. 2002 Jan 15;34(2):211-6.
3. Cui Q, S Shin W, Luo Y, Tian J, Cui H, Yin D. Thymidylate kinase: an old topic brings new perspectives. Current Medicinal Chemistry. 2013 Apr 1;20(10):1286-305.
4. Kotaka M, Dhaliwal B, Ren J, Nichols CE, Angell R, Lockyer M, Hawkins AR, Stammers DK. Structures of S. aureus thymidylate kinase reveal an atypical active site configuration and an intermediate conformational state upon substrate binding. Protein science. 2006 Apr;15(4):774-84.
5. Martínez-Botella G, Loch JT, Green OM, Kawatkar SP, Olivier NB, Boriack-Sjodin PA, Keating TA. Sulfonylpiperidines as novel, antibacterial inhibitors of Gram-positive thymidylate kinase (TMK). Bioorganic & medicinal chemistry letters. 2013 Jan 1;23(1):169-73.
6. Ostermann N, Schlichting I, Brundiers R, Konrad M, Reinstein J, Veit T, Goody RS, Lavie A. Insights into the phosphoryl transfer mechanism of human

thymidylate kinase gained from crystal structures of enzyme complexes along the reaction coordinate. Structure. 2000 Jun 1;8(6):629-42.

7. Jones TF, Creech CB, Erwin P, Baird SG, Woron AM, Schaffner W. Family outbreaks of invasive community-associated methicillin-resistant Staphylococcus aureus infection. Clinical Infectious Diseases. 2006 May 1;42(9):e76-8.
8. Jayanthi K, Azam MA. Thymidylate Kinase Inhibitors as Antibacterial Agents: A Review. Applied Biochemistry and Microbiology. 2023 Jun;59(3):250-66.
9. Munier-Lehmann HÉ, Charlotte A, Pochet S, Labesse G. Thymidylate kinase of Mycobacterium tuberculosis: a chimera sharing properties common to eukaryotic and bacterial enzymes. Protein Science. 2001 Jun;10(6):1195-205.
10. Ostermann N, Schlichting I, Brundiers R, Konrad M, Reinstein J, Veit T, Goody RS, Lavie A. Insights into the phosphoryl transfer mechanism of human thymidylate kinase gained from crystal structures of enzyme complexes along the reaction coordinate. Structure. 2000 Jun 1;8(6):629-42.
11. Martinez-Botella G, Breen JN, Duffy JE, Dumas J, Geng B, Gowers IK, Green OM, Guler S, Hentemann MF, Hernandez-Juan FA, Joseph-McCarthy D. Discovery of selective and potent inhibitors of gram-positive bacterial thymidylate kinase (TMK). Journal of medicinal chemistry. 2012 Nov 26;55(22):10010-21.
12. Jerez LB, Oyervides LR, Gómez A, Jiménez-Pérez VM, Muñoz-Flores BM. Electrochemical metallization with Sn of (E)-4-((4-nitrobenzylidene) amino) phenol in non-aqueous media: Characterization and biological activity of the organotin compound. Int. J. Electrochem. Sci. 2016;11:45-53.
13. Yele V, Azam MA, Wadhwani AD. Synthesis, Molecular Docking and Biological Evaluation of 2-Aryloxy-N-Phenylacetamide and N′-(2-Aryloxyoxyacetyl) Benzohydrazide Derivatives as Potential Antibacterial Agents. Chemistry & Biodiversity. 2021 Apr;18(4):e2000907.
14. Diniz-Neto H, Silva SL, Cordeiro LV, Silva DF, Oliveira RF, Athayde-Filho PF, Oliveira-Filho AA, Guerra FQ, Lima EO. Antifungal activity of 2-chloro-N-phenylacetamide: a new molecule with fungicidal and antibiofilm activity against fluconazole-resistant Candida spp. Brazilian Journal of Biology. 2022 Mar 9;84:e255080.

15. Dar AM, Mir S. Molecular docking: approaches, types, applications, and basic challenges. J Anal Bioanal Tech. 2017 Mar;8(2):1-3.
16. Madhavi Sastry G, Adzhigirey M, Day T, Annabhimoju R, Sherman W. Protein and ligand preparation: parameters, protocols, and influence on virtual screening enrichments. Journal of computer-aided molecular design. 2013 Mar;27:221-34.
17. Sukumaran Sunitha M. Meghna, Sneha S, Arjun B, Sathianarayanan S, Saranya T S. Insilico analysis of acridone against TNF-α and PDE4 targets for the treatment of psoriasis. Int. J. Res. Pharm. Sci. 2020;11:1251-9.
18. Dunkel M, Fullbeck M, Neumann S, Preissner R. SuperNatural: a searchable database of available natural compounds. Nucleic acids research. 2006 Jan 1;34(suppl_1):D678-83.
19. Roos K, Wu C, Damm W, Reboul M, Stevenson JM, Lu C, Dahlgren MK, Mondal S, Chen W, Wang L, Abel R. OPLS3e: Extending force field coverage for drug-like small molecules. Journal of chemical theory and computation. 2019 Feb 15;15(3):1863-74.
20. Jacobson MP, Pincus DL, Rapp CS, Day TJ, Honig B, Shaw DE, Friesner RA. A hierarchical approach to all-atom protein loop prediction. Proteins: Structure, Function, and Bioinformatics. 2004 May 1;55(2):351-67.
21. Guo Z, Mohanty U, Noehre J, Sawyer TK, Sherman W, Krilov G. Probing the α-helical structural stability of stapled p53 peptides: molecular dynamics simulations and analysis. Chemical biology & drug design. 2010 Apr;75(4):348-59.
22. Essmann U, Perera L, Berkowitz ML, Darden T, Lee H, Pedersen LG. A smooth particle mesh Ewald method. The Journal of Chemical Physics. 1995 Nov 15;103(19):8577-93.
23. Harder E, Damm W, Maple J, Wu C, Reboul M, Xiang JY, Wang L, Lupyan D, Dahlgren MK, Knight JL, Kaus JW. OPLS3: a force field providing broad coverage of drug-like small molecules and proteins. Journal of chemical theory and computation. 2016 Jan 12;12(1):281-96.
24. Martyna GJ, Tobias DJ, Klein ML. Constant pressure molecular dynamics algorithms. The Journal of Chemical Physics. 1994 Sep 1;101(5):4177-89.

25. Gupta SK, Singh AP, Karunakar M. Mesomorphic properties of benzoxazole Salicylaldimines and their Copper (II) Complexes: Synthesis and structural characterization. Results in Chemistry. 2022 Jan 1;4:100599.
26. Jacobs WA, Heidelberger M. METHODS FOR THE ACYLATION OF AROMATIC AMINO COMPOUNDS AND UREAS, WITH ESPECIAL REFERENCE TO CHLOROACETYLATION. Journal of the American Chemical Society. 1917 Jul;39(7):1439-47.
27. Lu Y, Chen J, Xiao M, Li W, Miller DD. An overview of tubulin inhibitors that interact with the colchicine binding site. Pharmaceutical research. 2012 Nov;29:2943-71.
28. Wayne PA. Clinical and Laboratory Standards Institute: Performance standards for antimicrobial susceptibility testing: 20th informational supplement. CLSI document M100-S20. 2010.
29. Ozturk S, Ercisli S. Chemical composition and in vitro antibacterial activity of Seseli libanotis. World Journal of Microbiology and Biotechnology. 2006 Mar;22:261-5.
30. Tsuji BT, Yang JC, Forrest A, Kelchlin PA, Smith PF. In vitro pharmacodynamics of novel rifamycin ABI-0043 against Staphylococcus aureus. Journal of Antimicrobial Chemotherapy. 2008 Jul 1;62(1):156-60.